Quantum Electronics **52** (6) 549–554 (2022)

https://doi.org/10.1070/QEL18066

CW optical parametric oscillator for the mid-IR range

M.D. Yakovin, P.L. Chapovsky

Abstract. **We report the development of a cw optical parametric oscillator (OPO) for the mid-IR range. The oscillator uses a 50-mm long periodically poled lithium niobate crystal in a ring resonator. The OPO is pumped by an ytterbium fibre laser with a wavelength of 1.064 μm. At a pump power of 10 W, the OPO generates continuous radiation with a wavelength of 3.6 μm and a power of 2.8 W. The pump power depletion in the OPO is 94%. The idler wave frequency of the OPO is stabilised using a precision laser wavelength meter. The rms error of the idler wave frequency in the stabilisation regime is 3 MHz. A simple theoretical model for the operation of a cw OPO is proposed, based on an empirical characteristic of the OPO, i.e., the pump depletion, and on a quantum description of three interacting light waves. The power characteristics of the operating OPO are in good agreement with those predicted by the theoretical model.**

Keywords: *cw optical parametric oscillator, mid-IR range, periodically poled $MgO:LiNbO_3$, theoretical model of a cw OPO.*

1. Introduction

Generation of coherent radiation by methods of nonlinear optics was discovered after the advent of lasers [1–5]. Second harmonic generation, parametric frequency conversion of coherent radiation, and many other nonlinear optical effects were discovered. To date, the methods of nonlinear optics have become an important alternative to the laser technique of generating coherent electromagnetic radiation, while they make it possible to successfully solve such problems of quantum electronics that are difficult or even impossible to solve by laser techniques.

One of these problems is to produce frequency-tunable radiation in the mid-IR range. In this case, of special value are sources of high-power cw infrared radiation, which is currently produced using optical parametric oscillators (OPOs). The difficulty of making cw OPOs is due to the need of using electromagnetic radiation with a high power density in order to achieve a high efficiency of nonlinear optical processes. High radiation powers in the OPO are achieved using optical resonators with a high quality factor at three, two or one of the three electromagnetic waves interacting with each other in the OPO. Single-resonant systems, which have a high quality factor for only one (signal) wave, have become most popular.

The first cw single-resonant OPO was reported in Ref. [6]. An important advantage of single-resonant OPOs is the relatively simple control of the frequency of the generated radiation. To date, many laboratory mid-IR OPOs have already been made; however, they still remain complex devices, and therefore further improvement of IR OPO designs is undoubtedly important. As far as we know, cw OPOs have not yet been made in our country, and spectroscopic studies in the mid-IR range have been carried out using pulsed OPOs [7–9].

The purpose of this work is to make a single-resonant cw OPO for the mid-IR range. The generator is supposed to be used to study the enrichment and conversion of nuclear spin isomers of polyatomic molecules by exciting rovibrational transitions of O–H and C–H bonds [10]. The paper is organised as follows. Section 2 presents a theoretical model of a cw OPO, Section 3 describes the experimental setup, Section 4 outlines the main characteristics of the newly developed OPO, and Section 5 summarises the main results of the work and draws conclusions.

2. Theoretical model of a cw OPO

The theory of cw OPOs is usually constructed by analogy with the theory of lasers [5, 11, 12]. It includes nonlinear optical wave gain coefficients, parameters of high-quality optical cavities, oscillation threshold, and other characteristics of an OPO. Models of this type are universal, but they are difficult to adapt to a quantitative description of real devices due to the complexity of measuring the characteristics of the OPO used in the theory. In this Section, we present a simple model of a cw OPO based on an easily measured empirical characteristic of the OPO, i.e. the pump depletion, which turns out to be an extremely informative characteristic of a cw OPO.

Nonlinear optics [3, 4, 11, 12] is based on the nonlinear dependence of the medium polarisation $\boldsymbol{P}$ on the electric field $\boldsymbol{E}$ of an electromagnetic wave:

$$P_i = \chi_{ij}^{(1)} E_j + \chi_{ijk}^{(2)} E_j E_k + \chi_{ijkl}^{(3)} E_j E_k E_l + \ldots . \quad (1)$$

Here the subscripts j, k, l denote the Cartesian components x, y, z of the quantities included in Eqn (1), and summation is performed over repeated subscripts. The linear susceptibility $\chi^{(1)}$ is responsible for the change in the refractive index of the medium, and the higher-order susceptibilities $\chi^{(2)}$, $\chi^{(3)}$, … are

M.D. Yakovin Institute of Automation and Electrometry, Siberian Branch, Russian Academy of Sciences, prosp. Akad. Koptyuga 1, 630090 Novosibirsk, Russia; e-mail: m.d.yakovin@mail.ru;
P.L. Chapovsky Institute of Automation and Electrometry, Siberian Branch, Russian Academy of Sciences, prosp. Akad. Koptyuga 1, 630090 Novosibirsk, Russia; Institute of Laser Physics, Siberian Branch, Russian Academy of Sciences, prosp. Akad. Lavrent'eva 15B, 630090 Novosibirsk, Russia; e-mail: chapovsky@iae.nsk.su

Received 22 March 2022, revision received 20 April 2022
Kvantovaya Elektronika **52** (6) 549–554 (2022)
Translated by E.N. Ragozin

responsible for the nonlinear interaction of waves according to the wave equation

$$\Delta \boldsymbol{E} - \frac{1}{c^2}\frac{\partial^2 \boldsymbol{E}}{\partial t^2} = \frac{4\pi}{c^2}\frac{\partial^2 \boldsymbol{P}}{\partial t^2}, \qquad (2)$$

where c is the speed of light in vacuum. The medium is assumed to be non-magnetic and without free electric charges. The nonlinear dependence of the polarisation on the electric field gives rise to the interaction of waves, the generation of new frequencies, and other nonlinear optical effects.

The nonlinear terms in Eqn (1) are small at the intensities of commonly available laser fields due to the smallness of the nonlinear susceptibilities. Therefore, in cw OPOs it is necessary to use two methods for enhancing nonlinear optical effects. Firstly, high intensities of light fields must be provided, which is achieved by focusing light beams and using high-quality resonators. Secondly, the phase-matched interaction of light waves in a long nonlinear crystal must be ensured. This phase-matched interaction occurs if the phase velocities of the nonlinear polarisation wave and its generated electromagnetic wave are equal to each other [see equations (1) and (2)].

The schematic of the OPO made in this work is shown in Fig.1. A periodically poled lithium niobate crystal is used in a bow-tie ring resonator. The resonator mirrors have a high reflection coefficient for the signal wave and a low one for the pump and idler waves. The OPO is designed to generate a high-power idler wave. The polarisation at the idler frequency

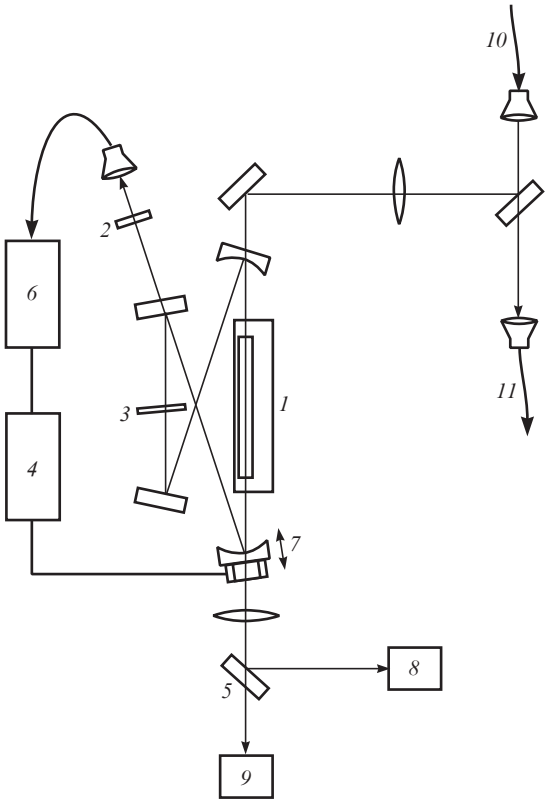

Figure 1. Schematic of the experimental setup:
(*1*) heater and crystal temperature stabilisation system; (*2*) idler wave radiation filter; (*3*) Fabry–Perot etalon; (*4*) piezoceramic control system; (*5*) dichroic mirror; (*6*) λ-meter of idle wave; (*7*) piezo stage; (*8*) pump power meter; (*9*) idler wave power meter; (*10*) optical fibre from the pump laser; (*11*) optical fibre to λ-meter of pump radiation.

is induced by the fields of the pump and signal waves. The pump wave passing through the crystal is partially converted into the idler and signal waves, which explains the importance of the pump wave power depletion for constructing a theoretical model of a cw OPO.

We consider the interaction of three monochromatic electromagnetic waves in a nonlinear medium underlying the operation of the OPO, which is due to the second-order nonlinear susceptibility $\chi^{(2)}$. Let us use a model of the process based on quantised optical fields. In the OPO, pump wave photons with frequency ω_p decay into signal and idler wave photons with frequencies ω_s and ω_i, respectively. The photons decay with the conservation of their energy:

$$\hbar\omega_p = \hbar\omega_s + \hbar\omega_i. \qquad (3)$$

The numbers of decayed pump photons and produced photons of the signal and idler waves are equal to each other,

$$n_p = n_s = n_i. \qquad (4)$$

This relation is a quantum interpretation of the Manley–Rowe theorem [13].

The laws of photon energy (3) and photon numbers (4) conservation for stationary monochromatic waves are fulfilled exactly. The momentum of photons during nonlinear conversion in the medium is conserved only approximately due to the spatially limited interaction of waves in the medium [11]. The change in momentum during the decay of a photon is equal to $\hbar\Delta\boldsymbol{k}$, where

$$\Delta\boldsymbol{k} = \boldsymbol{k}_p - \boldsymbol{k}_s - \boldsymbol{k}_i. \qquad (5)$$

Here $\boldsymbol{k}_p$, $\boldsymbol{k}_s$ and $\boldsymbol{k}_i$ are the wave vectors of the pump, signal, and idler waves in the medium. The nonlinear waves interaction is most effectively realised under phase matching, when $\Delta\boldsymbol{k} \approx 0$. In bulk crystals, the phase velocities of the nonlinear polarisation and its generated electromagnetic wave are equal to each other.

To achieve phase-matched wave interaction for $\Delta\boldsymbol{k} = 0$, advantage is taken of crystal birefringence and noncollinear wave propagation. In this case, it turns out to be very difficult to ensure phase-matched interaction of waves over large spatial intervals. It can be performed in periodically poled crystals, in which the sign of $\Delta\boldsymbol{k}$ is reversed in neighbouring domains. In such crystals, relation (5) takes on the following form for collinear waves [14]:

$$\Delta k_l = k_p - k_s - k_i - \frac{2\pi}{\Lambda}, \qquad (6)$$

where Λ is the spatial period of crystal polarisation. By varying the value of Λ, it is possible to realise the quasi-phase-matching condition with $\Delta k_l \approx 0$ and ensure efficient nonlinear interaction of light waves over large spatial intervals.

We determine the power characteristics that are important for the cw OPO developed in this work. These are: the pump radiation power P_p directed to the OPO; pump power depletion D_p, i.e. the fraction of the pump power converted into signal and idler waves; the signal wave power P_s accumulated in the OPO resonator; signal wave power D_s generated by the OPO; and the generated idler wave power D_i. The energy conservation law defines the relation $D_p = D_s + D_i$.

The above general information about the nonlinear interaction of three electromagnetic waves makes it possible to

obtain a number of important OPO characteristics. For example, expression (3) relates the frequencies and spectral widths of the pump, signal, and idler waves to each other. Since the numbers of decayed and born photons obey relation (4), the generated powers of the signal and idler waves of a cw OPO are determined as follows:

$$D_s = \hbar\omega_s \frac{D_p}{\hbar\omega_p}, \quad D_i = \hbar\omega_i \frac{D_p}{\hbar\omega_p}. \tag{7}$$

The polarisation of the nonlinear medium at the idler wave frequency is proportional to the product of the electric fields of the pump wave and the signal wave in the OPO resonator [see expression (1)]. Therefore, we can assume that the generated idler wave power D_i in a stationary OPO regime is approximately determined by the product of the pump power P_p and the signal wave power P_s accumulated in the resonator. This allows us to introduce the scaling parameter of a cw OPO

$$A = P_p P_s, \tag{8}$$

which has the dimensionality W^2. Varying the powers of the pump wave and the signal wave in the OPO resonator, while maintaining the scaling parameter A fixed, should keep constant the idler wave power D_i generated by the OPO.

The high intensity of the signal wave and the pump wave in the OPO resonator leads to nonuniform crystal heating and prevents the stable operation of the optical oscillator. The thermal power P_t released in the crystal is defined by the relation

$$P_t = \eta(P_p + P_s), \tag{9}$$

where η is the radiation-to-thermal power conversion efficiency. Here, for simplicity, we assumed that the crystal heating equally depends on the powers of both waves. Heating of the crystal by radiation can be minimised by varying the powers P_p and P_s, but at the same time retaining the value of the scaling parameter A and, consequently, the power of the generated idler wave D_i. Using relation (8), we represent the power of crystal heating by radiation in the form $P_t = \eta(P_p + A/P_p)$. Then the minimum crystal heating is achieved at $P_p = P_s = \sqrt{A}$, and the thermal power released in this case is $P_t = 2\eta\sqrt{A}$.

For clarity, let us numerically illustrate the decrease in crystal heating in an OPO by this method. Let the OPO have a pump power $P_p = 1$ W and a high-Q resonator providing the signal wave power in the resonator $P_s = 900$ W. For such an OPO, the scaling parameter is $A = 900$ W^2, and the crystal heating power is $P_t = \eta(P_p + P_s) = \eta 901$ W. In an OPO with a lower quality resonator chosen so that at a pump power $P_p = 30$ W the signal wave power $P_s = 30$ W, the scaling parameter A remains the same, but the crystal heating power decreases by a factor of 15 and becomes $P_t = \eta(P_p + P_s) = \eta 60$ W. A reduction of thermal effects in the OPO using a decrease in the power of the signal wave in the resonator was proposed in Ref. [15].

3. Experimental setup

The schematic of the experimental setup is shown in Fig. 1, and the photograph of the OPO ring resonator is shown in Fig. 2. The OPO is pumped by an YLR-50-1064-LP-SF ytterbium fibre laser (IPG Photonics) with a radiation wavelength of 1.064 μm, a laser linewidth of 40 kHz, and a maximum output power of 50 W. The pump radiation has a linear polarisation and a high beam quality ($M^2 = 1.07$). The laser is equipped with a Faraday isolator to protect against reflected radiation. The pump radiation is focused at the centre of the nonlinear OPO crystal by a single lens with a focal length of 200 mm.

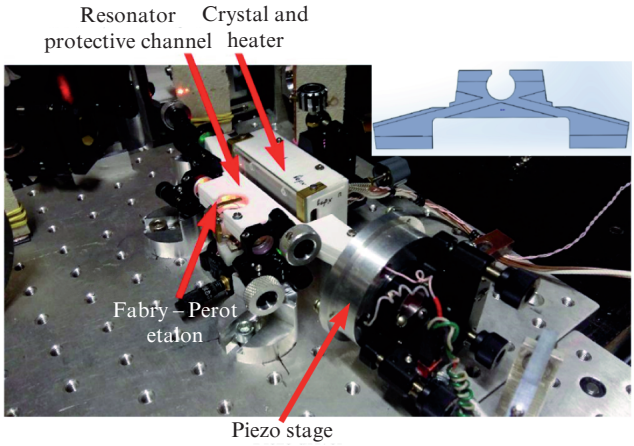

Figure 2. (Colour online) Photograph of the OPO ring resonator (top right, a protective channel for light beams in the OPO resonator).

The pump laser frequency was measured with a WS-U-10IR λ-meter (Angstrom, Novosibirsk), which has an absolute measurement accuracy of 10 MHz. From the dependence of the pump laser frequency on the time elapsed after it was turned on (Fig. 3), it follows that the laser must be switched on for a long time to achieve stable operation. Note that, according to expression (3), in order to obtain a stable idler wave frequency, the frequency deviation of the pump laser radiation can be compensated by appropriate tuning of the signal wave frequency.

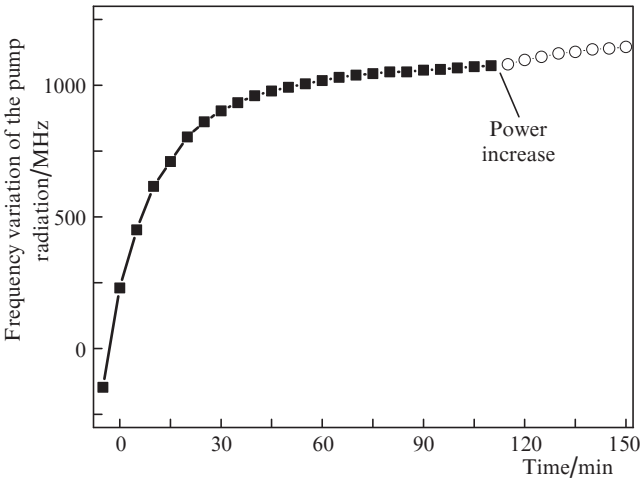

Figure 3. Dependence of the pump laser radiation frequency on the time elapsed after the laser was switched on.

The OPO ring resonator is formed by two spherical mirrors with curvature radii of 100 mm and a distance of 147 mm between them, as well as two plane mirrors with a distance of 56 mm between them. Resonator mirrors (Layertec, Germany) have a high reflection coefficient for the signal wave ($R >$ 99.9%) and low reflection coefficients for the pump wave ($R =$

0.5%) and idler wave ($R < 0.5\%$). The free spectral range (FSR) of the ring resonator is 636 MHz.

The OPO resonator design and the focusing of the pump radiation were carefully chosen on the basis of calculations using matrix optics for Gaussian beams. The confocal parameters of the pump and signal beams in the nonlinear crystal were 50 and 61 mm, respectively, and their calculated waist radii in the crystal were 63 and 83 μm, respectively.

In the OPO, we used a periodically poled magnesium oxide-doped lithium niobate crystal, MgO:PPLN (HC Photonics, Taiwan), measuring $50 \times 12.3 \times 1$ mm. The crystal contains ten polarisation gratings with periods from 27.6 to 31.6 μm. The face ends of the crystal were antireflection-coated for the pump wavelength and for a wide range of signal and idler wavelengths.

The stable operation of the OPO is possible only with precise (with an accuracy of ~1 mK) stabilisation of the crystal temperature [16]. We paid special attention to solving this problem. The nonlinear crystal was carefully thermally isolated from the environment, and its heating was provided by a precision electronic system of our special design. The crystal temperature was detected by a thermistor connected to the Wheatstone bridge circuit. The signal from the bridge was amplified by a high gain instrumentation amplifier and used to control the power section of the crystal heater. Note that in an operating OPO, the temperature of the crystal also depends on its heating by the pump radiation and the signal wave.

Stable OPO operation requires careful protection of its resonator from vibrations and air flows. In order to reduce vibrations, the OPO resonator was installed on a massive vibration-protected metal plate. The resonator was protected from air flows using a special channel with a small cross section, 5×6 mm, made with a 3D printer (see Fig. 2). This method of protection turned out to be more effective than a large enclosure around the entire OPO, which is used in all the works on optical parametric oscillators known to us. One of the advantages of the channel we used is that it leaves free access to all OPO adjustments.

The signal wave frequency is usually controlled using a Fabry–Perot etalon placed in the OPO resonator. For this purpose, we used a 1-mm-thick sapphire plane-parallel plate. Its transmittance versus radiation frequency (Fig. 4) was measured in a special experiment using a frequency-tunable semiconductor laser. The transmittance of the etalon at its maximum is, according to our measurements, 98.7%. To illustrate the selective capabilities of the Fabry–Perot etalon, Fig. 4 shows a frequency range approximately equal to the FSR of the OPO resonator.

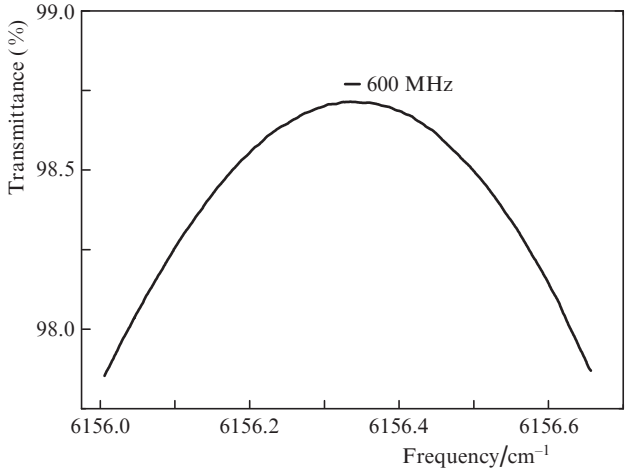

Figure 4. Transmittance of the Fabry–Perot etalon in relation to the radiation frequency. The label at the top is the intermode interval of the OPO resonator.

4. OPO characteristics

As an example, we outline the characteristics of the developed OPO using a pump power $P_p = 10$ W and an idler wave frequency of 2809 cm^{-1}. With a careful adjustment of the OPO resonator, the pump power converted into the signal and idler waves is 9.4 W. Thus, the pump power depletion is 94%. Relations (7) allow us to determine the calculated powers of the generated signal and idler waves:

$$D_s = 6.6 \text{ W}, D_i = 2.8 \text{ W}. \quad (10)$$

The generated power of the idle wave D_i is easy to measure experimentally, since the mirrors of the OPO resonator have a high transmittance for this wave. According to the measurements, the power of the idler wave

$$D_i = 2.8 \pm 0.2 \text{ W}, \quad (11)$$

which agrees well with the calculated value of D_i given above.

The calculated generated power of the signal wave is $D_s = 6.6$ W. In a stationary OPO, the entire power D_s must completely relax. One of the channels of signal wave relaxation is crystal heating. The electronic system for crystal temperature stabilisation made it possible to measure the radiation-related power of crystal heating, which amounted to 0.98 W. In Ref. [15], the absorption coefficient of a signal wave in an MgO:PPLN crystal was determined to be 0.08% cm^{-1} (i.e., 0.4% for our 5-cm long crystal). This means that the power in the resonator of our OPO is $P_s \approx 245$ W.

Other relaxation channels of signal wave power are transmission of OPO resonator mirrors, reflection from the Fabry–Perot etalon and from two surfaces of a nonlinear crystal. The power of the signal wave outgoing through the resonator mirrors can be easily measured directly. According to our measurements, for four resonator mirrors, it is 0.8 W. Therefore, (6.6 – 0.98 – 0.8) W ≈ 4.8 W remains in the balance of losses of the generated power of the signal wave. The reflection coefficient of the Fabry–Perot etalon is 1.3% (see Fig. 4), and the total reflection coefficient from the two ends of the crystal at the frequency of the signal wave is, according to our measurements, 0.48%. This means that the signal wave in the OPO resonator must have a power of ~270 W in order to ensure the 4.8-W power loss due to reflection from the Fabry–Perot etalon and the end surfaces of the crystal.

According to the above two estimates, the average power of the signal wave in the OPO resonator is $P_s \approx 260$ W. Therefore, at a pump power $P_p = 10$ W, the scaling parameter of the developed OPO is $A \approx 2.6 \times 10^3$ W^2. The intensity of the signal wave on the axis of the Gaussian beam at the centre of the crystal is approximately 2.4 MW cm^{-2}. The total loss of the signal wave in the OPO cavity is ~2.5%. Such relatively high losses help reduce the heating of the nonlinear crystal by radiation.

The frequency tuning of the idler wave in the constructed OPO can be carried out in several ways: by choosing the crys-

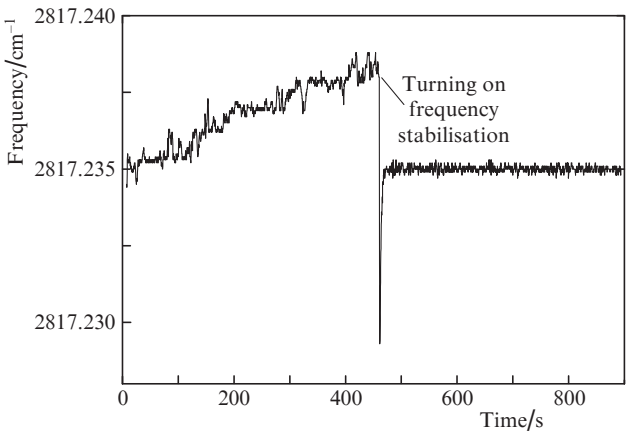

Figure 5. Temporal variation of the idler wave frequency in the free-running regime and in the frequency stabilisation regime using a WS-6-IR3 wavelength meter.

tal polarisation period, by changing the crystal temperature, by tilting the Fabry–Perot etalon in the resonator, and by changing the length of the ring resonator. The idler wave frequency was measured and stabilised in this work using a WS-6-IR3 λ-meter. Figure 5 shows the results of measuring the idler wave frequency in two OPO operation regimes: without stabilisation and with stabilisation of its frequency. In the former case, the idler wave frequency drifts due to the instability of the OPO parameters. When stabilisation is turned on, the frequency stops to drift. The root-mean-square error of the idler wave frequency is 3 MHz in this case. The absence of the idler wave frequency drift in the stabilisation regime means that it is determined by the drift of the λ-meter itself, and not by the OPO. Specifications of the λ-meter indicate that its frequency drift can be limited to ~10 MHz per day in a temperature-controlled room.

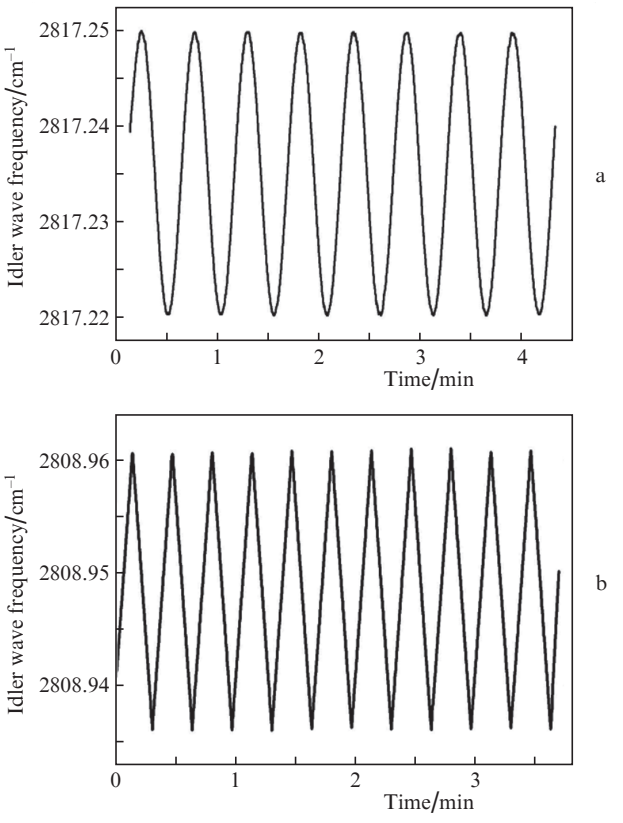

Figure 6. Idle wave frequency control according to (a) sinusoidal and (b) sawtooth laws.

The WS-6-IR3 λ-meter software permits stabilisation of the idler wave frequency not only to a constant value, but also to scan it according to the specified law. Scanning the frequency of the idle wave in time according to the sinusoidal and sawtooth laws is shown in Fig.6. When using the sinusoidal law, the frequency scanning range (Fig. 6) is 1.5 FSR of the OPO resonator. In our experiments, the frequency scanning range reached 2 FSRs, and the duration of stable idler frequency scanning was up to 23 min.

5. Main results

A cw OPO was developed for the mid-IR range, which makes it possible to obtain high-power monochromatic radiation in the range of 2.7–4 μm, within the range of the fundamental vibrational modes of the C–H and O–H bonds of polyatomic molecules. The OPO is pumped by ytterbium fibre laser radiation at a wavelength of 1.064 μm.

The oscillator has a bow-tie ring resonator and uses a periodically poled lithium niobate crystal of 50 mm length. For stable operation of the OPO, the crystal temperature was stabilised with an accuracy of ~1 mK using a special electronic temperature controller. To protect the OPO cavity from air flows, light beams were placed in a channel with a small cross section, which was printed by a 3D printer.

As an example, we outline the power characteristics of the OPO measured for an idler wave λ_i = 3.6 μm. At a pump power of 10 W, the pump depletion is 9.4 W, and the idler power reaches 2.8 ± 0.2 W. The power parameters of the OPO are close to the maximum possible limit. In particular, the depletion of the pump power is 94%, and the experimentally measured power of the idler wave coincides within the experimental uncertainty with the calculated power. According to our estimates, the power of the signal wave in the OPO resonator is ~260 W, while its intensity at the centre of the crystal on the beam axis amounts to ~2.4 MW cm^{-2}.

The idle wave frequency of the OPO was stabilised using a λ-meter WS-6-IR3 (Angstrem, Novosibirsk). The RMS error of the idler wave frequency in the stabilisation regime was 3 MHz. The possibility of smooth tuning of its frequency according to the sinusoidal and sawtooth laws was demonstrated. The range of smooth tuning of the idler wave frequency amounted to 2 FSRs of the OPO resonator.

A simple theoretical model of a cw OPO is proposed, which is based on an empirical OPO characteristic – the pump depletion value – and on a quantum description of three interacting light waves. The energy characteristics of the developed OPO are in good agreement with those predicted by the theoretical model.

Acknowledgements. The authors are very thankful to V.A. Akulov, M. Vainio, V.V. Vasiliev, S.L. Veber, D.B. Kolker, D.A. Radnatarov and V.A. Sorokin for useful discussions of the content of the paper.

This work was supported by the Russian Science Foundation (development of the experimental facility, Project No. 17-12-01418) and the Russian Ministry of Education and Science (development of the experimental facility, theoretical

analysis, projects AAAA-A21-121021800168-4 and AAAA-A19-119102890006-5).

References

1. Franken P.A., Hill A.E., Peters C.W., Weinreich G. *Phys. Rev. Lett*., **7**, 118 (1961).
2. Giordmaine J.A., Miller R.C. *Phys. Rev. Lett*., **14**, 973 (1965).
3. Akhmanov S.A., Khokhlov R.V. *Problems of Nonlinear Optics* (New York: Gordon and Breach, 1972; Moscow: Izd. AN SSSR, 1964).
4. Bloembergen N. *Nonlinear Optics* (New York: W.A.Benjamin, Inc., 1965) p. 135.
5. Harris S.E. *Proc. IEEE*, **57**, 2096 (1969).
6. Bosenberg W.R., Drobshoff A., Alexander J.I. *Opt. Lett.*, **21**, 1336 (1996).
7. Erushin E., Nyushkov B., Ivanenko A., Akhmathanov A., Shur V., Boyko A., Kostyukova N., Kolker D. *Laser Phys. Lett.*, **18**, 116201 (1921).
8. Kolker D.B., Sherstov I.V., Boyko A.A., Nyushkov B.N., Erushin E.Y., Kostyukova N.Y., Akhmathanov A.I., Kiryakova A.Y., Pavluck A.V. *J. Phys. Conf. Ser*., **2067**, 012013 (2021).
9. Antipov O.L., Kolker D.B., Dobrynin A.A., Getmanovskii Yu.A., Sharkov V.V., Chuvakova M.A., Akhmatkhanov A.R., Shur V.Ya., Shestakova I.A., Larin S.V. *Quantum Electron*., **52**, 254 (2022) [*Kvantovaya Elektron*., **52**, 254 (2022)].
10. Chapovsky P.L., Hermans L.J.F. *Annu. Rev. Phys. Chem*., **50**, 315 (1999).
11. Shen Y.R. *The Principles of Nonlinear Optics* (New-York: John Willey & Sons, Inc., 1984) p. 557.
12. Boyd R.W. *Nonlinear Optics* (United Kingdom: Academic Press, 2020).
13. Landau L.D., Lifshits E.M. *Electrodynamics of Continuous Media* (Oxford: Pergamon Press, 1960; Moscow: Nauka, 1992).
14. Myers L.E., Eckardt R.C., Fejer M.M., Byer R.L., Bosenberg W.R., Pierce J.W. *J. Opt. Soc. Am. B*, **12**, 2102 (1995).
15. Henderson A., Stafford R. *Appl. Phys. B*, **85**, 181 (2006).
16. Vainio M., Peltola J., Persijn S., Harren F.J.M., Halonen L. *Opt. Express*, **16**, 11141 (2008).